Special Issue

Impact of Choriocapillaris Flow on Multifocal Electroretinography in Intermediate Age-Related Macular Degeneration Eyes

Enrico Borrelli,[1] Rodolfo Mastropasqua,[2,3] Alfonso Senatore,[1] Michele Palmieri,[1] Lisa Toto,[1] SriniVas R. Sadda,[4,5] and Leonardo Mastropasqua[1]

[1]Ophthalmology Clinic, Department of Medicine and Science of Ageing, University G. D'Annunzio Chieti-Pescara, Chieti, Italy
[2]Whipps Cross University Hospital, Eye Treatment Centre, London, United Kingdom
[3]Ophthalmology Clinic, University of Marche, Ancona, Italy
[4]Doheny Image Reading Center, Doheny Eye Institute, Los Angeles, California, United States
[5]Department of Ophthalmology, David Geffen School of Medicine at UCLA, Los Angeles, California, United States

Correspondence: Enrico Borrelli, Ophthalmology Clinic, Department of Medicine and Science of Ageing, University G. D'Annunzio Chieti-Pescara, Via dei Vestini 31, 66100, Chieti, Italy; borrelli.enrico@yahoo.com.

Submitted: January 24, 2018
Accepted: April 25, 2018

Citation: Borrelli E, Mastropasqua R, Senatore A, et al. Impact of choriocapillaris flow on multifocal electroretinography in intermediate age-related macular degeneration eyes. *Invest Ophthalmol Vis Sci*. 2018;59:AMD25–AMD30. https://doi.org/10.1167/iovs.18-23943

Purpose. To investigate the relationship between perfusion of the choriocapillaris (CC) and macular function in eyes with intermediate age-related macular degeneration.

Methods. In this prospective, observational, cross-sectional study, macular optical coherence tomography angiography images and multifocal electroretinograms were obtained in 20 eyes with intermediate age-related macular degeneration from 20 patients. The main outcome measures were (1) the percent nonperfused choriocapillaris area (PNPCA), which represents a measure of the total area of CC vascular dropout, and (2) the average size of the CC signal voids, which represent contiguous regions of CC dropout. Furthermore, amplitude and implicit time of multifocal electroretinograms N1 and P1 waves in the two central rings (R1 and R2) were included in the analysis.

Results. Of the 20 patients enrolled, only 17 eyes from 17 patients (13 women) were included in this analysis. Three patients were excluded because of poor scan quality. Mean ± SD age was 75.1 ± 7.9 years (range, 62–89 years). The best corrected visual acuity was 0.17 ± 0.13 logarithm of the minimum angle of resolution. In univariate analysis, both the PNPCA and average signal void size were found to have a significant direct relationship with N1 implicit time in the R2 ring ($P = 0.006$ and $P = 0.035$, respectively). Neither PNPCA nor the average signal void size was associated with P1 or N1 implicit times in R1.

Conclusions. In intermediate age-related macular degeneration eyes, PNPCA and average signal void size are related to N1 multifocal electroretinogram implicit times, which suggests an association between CC perfusion and photoreceptor function.

Keywords: age-related macular degeneration, optical coherence tomography, electroretinogram

Intermediate age-related macular degeneration (iAMD) is clinically characterized by the accumulation of drusen and can progress to the late form of AMD notable for neovascularization or geographic atrophy.[1] Although late AMD is considered the leading cause of irreversible central vision loss among older individuals in developed countries, iAMD is often characterized by the conservation of a good level of visual acuity (VA).[2]

AMD is considered a complex disease with multifactorial etiologies. Although several factors have been involved in the pathogenesis and progression of this disorder,[3–5] a strong body of evidence suggests that AMD may be ultimately characterized by alterations of the photoreceptors, retinal pigment epithelium (RPE), Bruch's membrane, and choriocapillaris (CC) complex.[5,6] The CC is a labyrinth of thin-walled and fenestrated capillaries distinguished by a high flow rate, which is essential to deliver enough oxygen by diffusion to photoreceptors and maintain the oxidative metabolism driving phototransduction. Thus, it seems rational that a reduction in CC flow may affect structure and function of photoreceptors.

Optical coherence tomography angiography (OCTA) has provided the capability to evaluate the retinal and anterior choroidal vascular circulations without the need for dye injection.[7–10] Previous dye-based techniques have some significant limitations for the evaluation of the CC, and thus OCTA may become a key technology for the in vivo evaluation of the CC. In the OCTA CC scans, dark regions referred to as flow voids may alternate with granular bright areas, and this pattern may systematically change with age or myopia.[11,12] It is important to note that the detectable flow range of OCTA is limited and flows below the slowest detectable motion produce decorrelations that are indistinguishable from background noise.[13] Considering this, CC flow voids have recently been renamed signal voids.[14] With advanced image processing software, quantification of the total number and the total and average area of these CC signal voids is now possible.[11,14]

Previous studies used the best corrected VA (BCVA) to evaluate the macular function in iAMD eyes.[15] Nevertheless, the introduction of the multifocal electroretinogram (mfERG) has allowed clinicians to test the whole macular function and to study morpho-functional correlations in eyes affected by AMD.[16–18]

The main aim of this study was to explore the relationship between the CC perfusion and macular function in iAMD eyes as assessed by mfERG.

Methods

Study Participants

In this prospective, observational, cross-sectional study, patients 50 years of age and older with iAMD in at least one eye were enrolled at the ophthalmology clinic of University G. d'Annunzio, Chieti-Pescara, Italy. The study was approved by the institutional review board and adhered to the tenets of the Declaration of Helsinki. An informed consent approved by the institutional review board was obtained from all patients.

All patients enrolled were imaged with the RTVue XR Avanti AngioVue OCTA (Optovue, Inc., Fremont, CA, USA) between October 2016 and June 2017. Moreover, all patients received a complete ophthalmologic examination, which included the measurement of Snellen BCVA, IOP, and dilated ophthalmoscopy.

The inclusion criteria for iAMD eyes included the presence of drusen >125 μm in diameter with or without pigmentary abnormalities as assessed by clinical examination and confirmed by dense volume optical coherence tomography (OCT) (pigment abnormalities on OCT manifesting as intraretinal hyper-reflective features).[1] Exclusion criteria for iAMD eyes were (1) pseudodrusen on the OCT scan, because of their presence have been shown to influence both CC perfusion[15] and mfERG values[19]; (2) previous ocular surgery or history of antivascular endothelial growth factor therapy; (3) any maculopathy secondary to causes other than AMD (including the presence of an epiretinal membrane or vitreomacular traction syndrome); (4) the presence of significant media opacities; (5) myopia greater than −3.00 diopters; and (6) any optic neuropathy, including glaucoma. Furthermore, images with a strength index less than 40, with either significant motion artifact (seen as large dark lines on the en face angiogram) or incorrect segmentation at the level of the CC were excluded from the analysis.

Imaging

Patients underwent OCTA imaging using the RTVue XR Avanti spectral-domain OCT device with AngioVue software (version 2016.1.0.26; Optovue, Inc.), which is based on a split-spectrum amplitude-decorrelation angiography algorithm. Flow is detected as a variation of amplitude over time in the speckle pattern formed by the interference of light scattered from red blood cells and adjacent tissue structures.[20] For each patient, a 3 × 3-mm cube scan was acquired containing 304 × 304 A-scans.

Image Processing

The main outcome measures were (1) the percent non-perfused choriocapillaris area (PNPCA), which represents a measure of the total area of CC vascular dropout, and (2) the average size of the CC signal voids, the latter representing contiguous regions of CC dropout.

To evaluate the PNPCA and the average signal void size, we analyzed the images as already described.[15,21,22] In brief, the PNPCA was computed as the percentage of pixels in the CC en face image (slab 30-μm thick starting 31 μm posterior to the RPE reference) below a "non-perfusion" (or noise) threshold, which was calculated with ImageJ software version 1.50 (National Institutes of Health, Bethesda, MD, USA; http://rsb.info.nih.gov/ij/index.html) as the mean of all the pixel values in the outer avascular retina. The PNPCA was thus calculated as the number of pixels falling below the threshold (the total area of the signal voids) divided by the total number of pixels in the analyzed area of CC. Furthermore, the "Analyze Particles" command, which measured and counted all thresholded areas greater or equal to 1 pixel where there was a lack of flow information, furnished us the average size of the signal voids.

Notably, the CC directly beneath drusen, as well as under superficial retinal vessels, was excluded from the analysis to avoid shadowing or projection artifacts from confounding the analysis, as already shown (Fig. 1).[21,22] In brief, the drusen area was identified on the "RPE elevation" map elaborated by the AngioVue software. This image was imported into ImageJ, and the "Split Channels" function was carried on to obtain the "green channel" image. In the latter image, the RPE elevation area appears darker then the surrounding area, and the "MaxEntropy" threshold was therefore applied to "binarize" the obtained image. The superficial capillary plexus (SCP) en face OCTA image was segmented with an inner boundary 3 μm below the internal limiting membrane and an outer boundary set at 15 μm below the inner plexiform layer. The en face SCP image was opened in ImageJ, and the "MaxEntropy" threshold was applied to visualize only the greater superficial retinal vessels (causing shadowing and artifacts). The three obtained images (CC en face image and images identifying superficial vessels and drusen regions) were merged to mask those regions beneath drusen and/or superficial vessels.

Multifocal Electroretinogram (mfERG)

mfERG (Retimax CSO, Florence, Italy) was recorded for each patient according to the International Society for Clinical Electrophysiology of Vision protocol that was updated in 2011.[23] Pupils were dilated with 1% tropicamide and recording began only when the pupils were dilated to at least 7 mm. Because retinal adaptation may affect mfERG results, the patients were exposed at the same preexposure light and the illumination in the examination room was moderate and the same for all patients, as previously suggested.[23] At each mfERG examination, patients positively reported that he/she could clearly perceive the fixation target. Moreover, the eye's position was monitored by a video system. During the mfERG examination, the ocular fundus was segmented by an array of 61 hexagons. The amplitudes and implicit times of N1 (first negative component) and P1 (first positive component) of the first-order kernel were calculated for five regional ring groups (R1, R2, R3, R4, and R5). The amplitude of N1 was measured from the baseline to the first negative peak. The P1's amplitude was measured from the first negative peak to the first positive peak. The latencies were defined as the time period from the stimulus onset to the peak of N1 and P1 responses.

The responses from the central two rings were included in the analysis, where rings R1 and R2 cover areas approximately 0° to 5° and 6° to 10°, respectively, from the fovea. This choice was made because these two rings overlay a 2.8-mm-diameter circle area centered on the fovea, similar to the filed covered by the OCTA scan (Figs. 2, 3).

Statistical Analysis

Statistical calculations were performed using Statistical Package for Social Sciences (version 20.0, SPSS, Inc., Chicago, IL, USA). To detect departures from normality distribution, Shapiro-Wilk's test was performed for all variables. All quantitative variables were presented as mean and SD in the results.

Investigative Ophthalmology & Visual Science

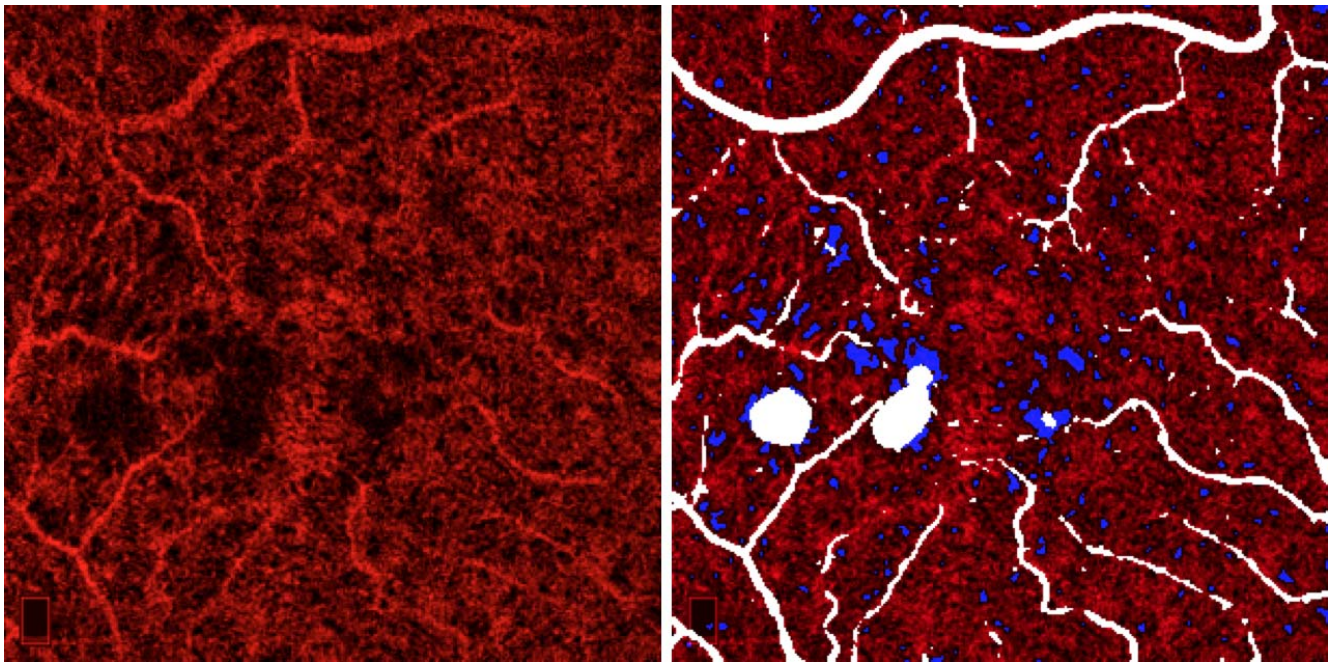

FIGURE 1. Representative optical coherence tomography angiography (OCTA) 3 × 3-mm scan segmented at the choriocapillaris (CC) plexus from an intermediate AMD (iAMD) patient (*left*). The area beneath drusen and superficial retinal vessels was masked (*white area* in the *right* image). The percent of nonperfused choriocapillaris area (PNPCA) was obtained by dividing the area below the nonperfusion threshold (*blue dots*) by the remaining area of CC.

Univariate regression analyses of potential associations between the OCTA and functional parameters were performed. For each analysis, a standardized β coefficient was calculated. This compares the strength of the effect of each individual independent variable to the dependent variable. The higher the absolute value of the standardized β coefficient (values between 0 and ± 1), the stronger the effect.

The BCVA for each eye was converted to the logarithm of the minimum angle of resolution, as previously described.[24]

The chosen level of statistical significance was $P < 0.05$.

RESULTS

Characteristics of Patients Included in the Analysis

Of the 20 patients enrolled, only 17 eyes from 17 patients (13 women) were included in this analysis. Three patients were excluded because of poor scan quality. Mean ± SD age was 75.1 ± 7.9 years (range, 62–89 years). The BCVA was 0.17 ± 0.13 logarithm of the minimum angle of resolution.

mfERG N1 and P1 amplitudes were –0.38 ± 0.30 and 0.50 ± 0.35 μV, and –0.22 ± 0.13 and 0.49 ± 0.25 μV, in the R1 and R2 rings, respectively.

mfERG N1 and P1 implicit times were 18.6 ± 2.4 milliseconds and 38.2 ± 2.1 milliseconds in R1, 16.5 ± 3.9 milliseconds and 36.2 ± 2.3 milliseconds in R2.

In the OCTA evaluation of the CC layer, the whole PNPCA was 4.1 ± 2.0%, the average signal void size was 281.7 ± 65.4 μm^2, and the average signal void number was 1225.2 ± 336.3, respectively. Topographically, the PNPCA in the 1.4-mm-wide circle centered on the fovea was 5.2 ± 12.0% of the whole PNPCA in the 3 × 3-mm-wide scan.

Regression Analysis

In univariate analysis (Table), both the PNPCA and average signal void size were found to have a significant direct relationship with N1 implicit time in the R2 ring ($P = 0.006$ and $P = 0.035$, respectively). In R1, the average signal void size was statistically associated with N1 amplitude ($P = 0.015$). Neither the PNPCA nor the average signal void size was

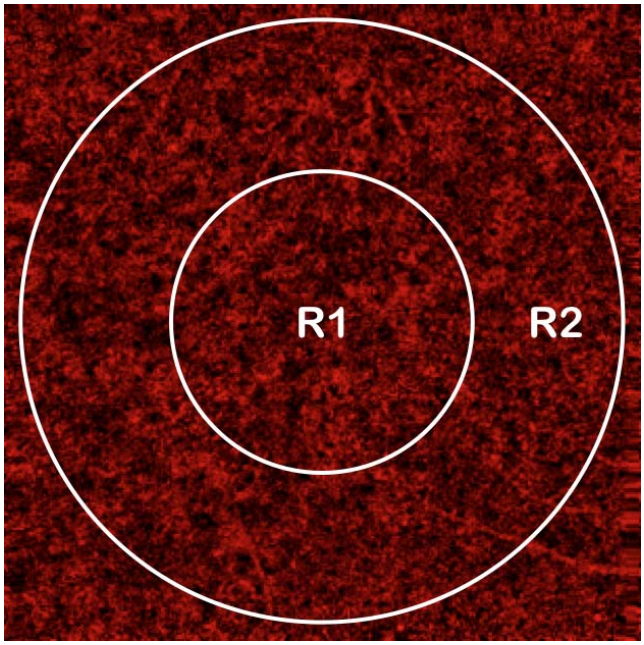

FIGURE 2. Representative optical coherence tomography angiography (OCTA) 3 × 3-mm image of the choriocapillaris (CC). The macular function was investigated using multifocal electroretinogram (mfERG) in the central two rings (R1 and R2), where rings R1 and R2 cover areas approximately 0° to 5° and 6° to 10°, respectively, from the fovea. This choice was made because these two rings overlay a 2.8-mm-diameter circle area centered on the fovea, similar to the filed covered by the OCTA scan.

Table. Univariate Analysis Between Optical Coherence Tomography Angiography and Multifocal Electroretinogram Parameters

	PNPCA		Average Signal Void Size		Average Signal Void Number	
Tested Variables	Standardized β Coefficient	*P*	Standardized β Coefficient	*P*	Standardized β Coefficient	*P*
R1N1A	−0.340	0.182	−0.579	**0.015**	−0.094	0.718
R1P1A	−0.050	0.849	−0.241	0.352	−0.007	0.980
R1N1L	0.015	0.956	−0.019	0.943	0.077	0.770
R1P1L	−0.291	0.257	−0.259	0.316	−0.261	0.312
R2N1A	−0.401	0.201	−0.478	0.115	−0.098	0.712
R2P1A	0.405	0.112	0.370	0.143	0.423	0.091
R2N1L	0.639	**0.006**	0.512	**0.035**	0.394	0.117
R2P1L	0.116	0.650	0.347	0.173	0.342	0.179

Standardized β coefficient comprised between 0 and ±1. The higher the absolute value is, the stronger is the association between the two variables. Significant *P* values (<0.05) are in bold. OCTA, optical coherence tomography angiography; PNPCA, percent nonperfused choriocapillaris area; R1N1A, first negative component amplitude in the first ring; R1P1A, first positive component amplitude in the first ring; R1N1L, first negative component implicit time in the first ring; R1P1L, first positive component implicit time in the first ring; R2N1A, first negative component amplitude in the second ring; R1P1A, first positive component amplitude in the second ring; R1N1L, first negative component implicit time in the second ring; R1P1L, first positive component implicit time in the second ring.

associated with P1 or N1 implicit times in R1. OCTA values were not associated with BCVA ($P > 0.05$ for all univariate analyses).

Discussion

In this prospective, cross-sectional study we investigated CC features and macular function in iAMD eyes. Overall, we found that the PNPCA was associated with changes in mfERG implicit time, but not mfERG response amplitudes.

In recent years, OCTA technology has been shown to be useful in studying AMD eyes. Several studies assessed the retinal and choroidal vasculature in eyes with iAMD and showed that iAMD eyes are characterized by a reduced SCP and CC perfusion density, especially in the presence of nascent geographic atrophy or neovascularization in the fellow eye.[21,25–28] The average signal void size of the CC and PNPCA were recently characterized in eyes with iAMD using spectral domain optical coherence tomography angiography.[21] In the latter study, OCTA data from 42 iAMD eyes (42 patients) and 20 eyes from 20 healthy individuals were retrospectively collected. The iAMD cohort was divided into two subgroups according to the status of the fellow eye, yielding a group of 20 cases with bilateral iAMD and 22 cases with neovascular AMD in the fellow eye (unilateral iAMD). Interestingly, the CC was demonstrated to be more affected in intermediate AMD eyes with neovascular AMD in the fellow eye.

The measurement of macular function using mfERG has been suggested to be useful in the assessment of early/intermediate AMD eyes, as several notable studies have reported that functional alterations can be effectively detected using this technique.[29–33] A comparison in macular function measured using mfERG with microperimetry in iAMD eyes was reported by Wu et al.,[34] who showed that the measured functional deficit with microperimetry was greater than with mfERG. Furthermore, they found a lack of correlation between these two functional measures, suggesting that mfERG may evaluate unique aspects of macular dysfunction. The mfERG is indeed considered as an electrophysiological measure of suprathreshold postreceptoral responses at photopic levels, which mainly originate from the cone photoreceptors,[35] whereas microperimetry is a measure of sensitivity at mesopic levels, which may be mediated by both rod and cone photoreceptor pathways.[36]

The macular sensitivity in iAMD eyes was also tested by Gerth and colleagues,[30] who demonstrated functional changes in the cone-driven pathway, as evaluated by mfERG, especially with regard to implicit times, which were shown to be altered beyond the visible drusen area. Interestingly, mfERG implicit times were demonstrated to have a progressive worsening despite stable VA.[29]

Wu et al.[37] investigated the association between macular function by mfERG and photoreceptor damage, which was assessed by analyzing the inner segment/outer segment (IS/OS) junction reflectivity with OCT. The reflection signal arising from IS/OS junction has been suggested to originate from the photoreceptor IS ellipsoids.[38] Because discontinuities in the IS/OS junction are seen as hyporeflective areas on the en face image, it has been demonstrated that the reflectivity of the IS/OS junction might be a surrogate for photoreceptor damage.[39–41] Wu et al.[37] demonstrated a significant negative association between IS/OS reflectivity and mfERG values, which may suggest that the mfERG responses are influenced by the photoreceptor loss.

The mfERG macular function in early/intermediate AMD eyes was also studied by Parisi et al.,[32] who enrolled 27 patients and assessed the influence of short-term carotenoid and antioxidant supplementation on macular function. In this study, the authors demonstrated that a selective dysfunction in the macula may be improved by this supplementation.

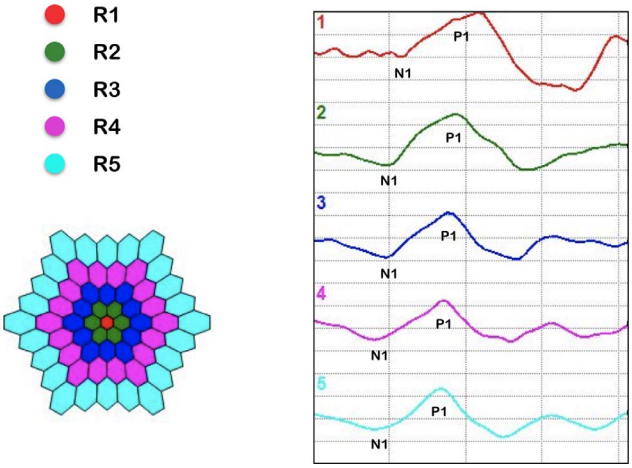

Figure 3. Multifocal electroretinogram of a patient affected by intermediate AMD. Amplitudes and latencies of N1 (first negative component) and P1 (first positive component) of the first-order kernel were recorded for five regional ring groups (R1, R2, R3, R4, and R5). Data of the first two rings (R1 and R2) were included in the analysis.

Two previous notable studies have investigated the association between the CC perfusion and VA in iAMD eyes.[15,21] Both studies did not find a correlation between these two parameters in iAMD eyes without pseudodrusen, as confirmed in our results. Interestingly, Nesper et al.[15] demonstrated that the PNPCA was negatively correlated with VA only in those iAMD eyes with pseudodrusen. However, given that AMD is a disorder that affects regions beyond the foveola, the functional information provided by VA is limited.[42] Furthermore, VA is highly dependent on fixation, which may also be compromised in AMD.[43]

We add to the literature by reporting the association between CC perfusion and macular function. We found that N1 mfERG implicit time was associated with increased PNPCA and average signal void size. Because the N1 wave is thought to generate from the postreceptoral signals after cones (it is indeed mainly shaped by the initial hyperpolarization of the OFF-bipolar cells), whereas the P1 wave is known to be more influenced by the inner retina, we speculate that the CC changes may affect the postphotoreceptor function. Interestingly, we found that this association was significant only in the R2 ring. This aspect may be explained by the topographical features of AMD, which may affect the parafoveal region more extensively in its early or intermediate stages.[42] Furthermore, although we demonstrated that the CC dropout was mainly located in the parafoveal region, this aspect may also explain the absence of association in R1.

Furthermore, the association between CC changes and mfERG implicit time, but not response amplitude, suggests an association with neuroretinal functional abnormalities of the photoreceptor-mediated pathway rather than cell loss.[17] However, our findings are unable to determine the exact mechanisms responsible for these functional changes. Prospective longitudinal studies will help shed further light on the relation between CC perfusion and macular function.

Our study has some limitations. The study sample was relatively small and we did not enroll healthy individuals for comparison. However, the aim of this study was to assess the presence of an association between CC perfusion and macular function because other studies have already investigated these OCTA parameters in iAMD and healthy eyes. In addition, this study was not large enough to account for confounding factors such as age, diabetes, or smoking, which are known to affect electroretinogram values.[44–46] Furthermore, shifts in fixation may have been a limitation in examining the association between the pathological features and functional changes in the central macular region. Nevertheless, the fixation monitoring system used during mfERG recordings allowed us to assess the occurrence of any contamination by blinks or eye movements. Also, the study was not large enough to account for confounding factors such as age, diagnosis of diabetes, smoking status, gender, or drusen volume. Finally, we did not investigate the microperimetry or contrast sensitivity in our study cohort.

In conclusion, despite these limitations, this study investigated the relationship between CC perfusion and mfERG macular function in eyes with intermediate AMD. We observed that the PNPCA and average signal void size are related to N1R2 mfERG implicit times, which suggests an association between CC perfusion and postphotoreceptor function rather than cell loss. These findings may help broaden our knowledge regarding the pathophysiology and evolution of AMD.

Acknowledgments

Disclosures: **E. Borrelli**, None; **R. Mastropasqua**, None; **A. Senatore**, None; **M. Palmieri**, None; **L. Toto**, None; **S.R. Sadda**, Allergan (C, F), Carl Zeiss Meditec (F), Genentech (C, F), Iconic (C), Novartis (C), Optos (C,F), Optovue (C, F), Regeneron (F), Thrombogenics (C); **L. Mastropasqua**, None

References

1. Ferris FL, Wilkinson CP, Bird A, et al. Clinical classification of age-related macular degeneration. *Ophthalmology*. 2013;120:844–851.
2. Friedman DS, O'Colmain BJ, Muñoz B, et al. Prevalence of age-related macular degeneration in the United States. *Arch Ophthalmol*. 2004;122:564–572.
3. Klein R, Myers CE, Cruickshanks KJ, et al. Markers of inflammation, oxidative stress, and endothelial dysfunction and the 20-year cumulative incidence of early age-related macular degeneration. *JAMA Ophthalmol*. 2014;132:446.
4. Saksens NTM, Geerlings MJ, Bakker B, et al. Rare genetic variants associated with development of age-related macular degeneration. *JAMA Ophthalmol*. 2016;134:287.
5. Querques G, Rosenfeld PJPJ, Cavallero E, et al. Treatment of dry age-related macular degeneration. *Ophthalmic Res*. 2014;52:107–115.
6. Zarbin MA, Rosenfeld PJ. Pathway-based therapies for age-related macular degeneration: an integrated survey of emerging treatment alternatives. *Retina*. 2010;30:1350–1367.
7. Kuehlewein L, Sadda SR, Sarraf D. OCT angiography and sequential quantitative analysis of type 2 neovascularization after ranibizumab therapy. *Eye*. 2015;29:932–935.
8. Kuehlewein L, Bansal M, Lenis TL, et al. Optical coherence tomography angiography of type 1 neovascularization in age-related macular degeneration. *Am J Ophthalmol*. 2015;160:739–748.e2.
9. Moult E, Choi W, Waheed NK, et al. Ultrahigh-speed swept-source OCT angiography in exudative AMD. *Ophthalmic Surg Lasers Imaging Retina*. 2014;45:496–505.
10. Mastropasqua L, Toto L, Borrelli E, Carpineto P, Di Antonio L, Mastropasqua R. Optical coherence tomography angiography assessment of vascular effects occurring after aflibercept intravitreal injections in treatment-naive patients with wet AMD. *Retina*. 2017;37:247–256.
11. Spaide RF. Choriocapillaris flow features follow a power law distribution: implications for characterization and mechanisms of disease progression. *Am J Ophthalmol*. 2016;170:58–67.
12. Al-Sheikh M, Phasukkijwatana N, Dolz-Marco R, et al. Quantitative OCT angiography of the retinal microvasculature and the choriocapillaris in myopic eyes. *Invest Ophthalmol Vis Sci*. 2017;58:2063–2069.
13. Choi W, Moult EM, Waheed NK, et al. Ultrahigh-speed, swept-source optical coherence tomography angiography in non-exudative age-related macular degeneration with geographic atrophy. *Ophthalmology*. 2015;122:2532–2544.
14. Spaide RF. Choriocapillaris signal voids in maternally inherited diabetes and deafness and in pseudoxanthoma elasticum. *Retina*. 2017;37:2008–2014.
15. Nesper PL, Soetikno BT, Fawzi AA. Choriocapillaris nonperfusion is associated with poor visual acuity in eyes with reticular pseudodrusen. *Am J Ophthalmol*. 2017;174:42–55.
16. Toto L, Borrelli E, Mastropasqua R, et al. Macular features in retinitis pigmentosa: correlations among ganglion cell complex thickness, capillary density, and macular function. *Invest Opthalmology Vis Sci*. 2016;57:6360.
17. Hood DC. Assessing retinal function with the multifocal technique. *Prog Retin Eye Res*. 2000;19:607–646.
18. Hood DC, Raza AS, de Moraes CGV, Liebmann JM, Ritch R. Glaucomatous damage of the macula. *Prog Retin Eye Res*. 2013;32:1–21.

19. Wu Z, Ayton LN, Makeyeva G, Guymer RH, Luu CD. Impact of reticular pseudodrusen on microperimetry and multifocal electroretinography in intermediate age-related macular degeneration. *Invest Ophthalmol Vis Sci*. 2015;56:2100–2106.
20. Jia Y, Tan O, Tokayer J, et al. Split-spectrum amplitude-decorrelation angiography with optical coherence tomography. *Opt Express*. 2012;20:4710–4725.
21. Borrelli E, Uji A, Sarraf D, Sadda SR. Alterations in the choriocapillaris in intermediate age-related macular degeneration. *Invest Opthalmology Vis Sci*. 2017;58:4792–4798.
22. Borrelli E, Lonngi M, Balasubramanian S, et al. Macular microvascular networks in healthy pediatric subjects [published online ahead of print February 22, 2018]. *Retina*. https://doi.org/10.1097/IAE.0000000000002123.
23. Hood DC, Bach M, Brigell M, et al. ISCEV standard for clinical multifocal electroretinography (mfERG) (2011 edition). *Doc Ophthalmol*. 2012;124:1–13.
24. Holladay JT. Proper method for calculating average visual acuity. *J Refract Surg*. 1997;13:388–391.
25. Toto L, Borrelli E, Mastropasqua R, et al. Association between outer retinal alterations and microvascular changes in intermediate stage age-related macular degeneration: an optical coherence tomography angiography study. *Br J Ophthalmol*. 2017;101:774–779.
26. Moult EM, Waheed NK, Novais EA, et al. Swept-source optical coherence tomography angiography reveals choriocapillaris alterations in eyes with nascent geographic atrophy and drusen-associated geographic atrophy. *Retina*. 2016;36:S2–S11.
27. Toto L, Borrelli E, Di Antonio L, Carpineto P, Mastropasqua R. Retinal vascular plexuses' changes in dry age-related by means of optical coherence. *Retina*. 2016;36:1566–1572.
28. Borrelli E, Souied EH, Freund KB, et al. Reduced choriocapillaris flow in eyes with type 3 neovascularization due to age-related macular degeneration subjects [published online ahead of print April 30, 2018]. *Retina*. doi:10.1097/IAE.0000000000002198.
29. Gerth C, Hauser D, Delahunt PB, Morse LS, Werner JS. Assessment of multifocal electroretinogram abnormalities and their relation to morphologic characteristics in patients with large drusen. *Arch Ophthalmol*. 2003;121:1404–1414.
30. Gerth C, Delahunt PB, Alam S, Morse LS, Werner JS. Cone-mediated multifocal electroretinogram in age-related macular degeneration: progression over a long-term follow-up. *Arch Ophthalmol*. 2006;124:345–352.
31. Li J, Tso MO, Lam TT. Reduced amplitude and delayed latency in foveal response of multifocal electroretinogram in early age related macular degeneration. *Br J Ophthalmol*. 2001;85:287–290.
32. Parisi V, Tedeschi M, Gallinaro G, et al. Carotenoids and antioxidants in age-related maculopathy italian study: multifocal electroretinogram modifications after 1 year. *Ophthalmology*. 2008;115:324–333.e2.
33. Parisi V, Perillo L, Tedeschi M, et al. Macular function in eyes with early age-related macular degeneration with or without contralateral late age-related macular degeneration. *Retina*. 2007;27:879–890.
34. Wu Z, Ayton LN, Guymer RH, Luu CD. Comparison between multifocal electroretinography and microperimetry in age-related macular degeneration. *Invest Ophthalmol Vis Sci*. 2014;55:6431–6439.
35. Hood DC, Frishman LJ, Saszik S, Viswanathan S. Retinal origins of the primate multifocal ERG: implications for the human response. *Invest Ophthalmol Vis Sci*. 2002;43:1673–1685.
36. Tepelus TC, Hariri AH, Al-Sheikh M, Sadda SR. Correlation between mesopic retinal sensitivity and optical coherence tomographic metrics of the outer retina in patients with non-atrophic dry age-related macular degeneration. *Ophthalmic Surg Lasers Imaging Retina*. 2017;48:312–318.
37. Wu Z, Ayton LN, Guymer RH, Luu CD. Relationship between the second reflective band on optical coherence tomography and multifocal electroretinography in age-related macular degeneration. *Invest Opthalmology Vis Sci*. 2013;54:2800–2806.
38. Staurenghi G, Sadda SR, Chakravarthy U, Spaide RF; International Nomenclature for Optical Coherence Tomography (IN•OCT) Panel. Proposed lexicon for anatomic landmarks in normal posterior segment spectral-domain optical coherence tomography: the IN•OCT consensus. *Ophthalmology*. 2014;121:1572–1578.
39. Hood DC, Zhang X, Ramachandran R, et al. The inner segment/outer segment border seen on optical coherence tomography is less intense in patients with diminished cone function. *Invest Opthalmology Vis Sci*. 2011;52:9703–9709.
40. Pappuru RR, Ouyang Y, Nittala MG, et al. Relationship between outer retinal thickness substructures and visual acuity in eyes with dry age-related macular degeneration. *Invest Ophthalmol Vis Sci*. 2011;52:6743–6748.
41. Borrelli E, Abdelfattah NS, Uji A, Nittala MG, Boyer DS, Sadda SR. Postreceptor neuronal loss in intermediate age-related macular degeneration. *Am J Ophthalmol*. 2017;181:1–11.
42. Curcio CA. Photoreceptor topography in ageing and age-related maculopathy. *Eye*. 2001;15:376–383.
43. Bellmann C, Feely M, Crossland MD, Kabanarou SA, Rubin GS. Fixation stability using central and pericentral fixation targets in patients with age-related macular degeneration. *Ophthalmology*. 2004;111:2265–2270.
44. Celesia GG, Kaufman D, Cone S. Effects of age and sex on pattern electroretinograms and visual evoked potentials. *Electroencephalogr Clin Neurophysiol*. 1987;68:161–171.
45. Bearse MA, Adams AJ, Han Y, et al. A multifocal electroretinogram model predicting the development of diabetic retinopathy. *Prog Retin Eye Res*. 2006;25:425–448.
46. Gundogan FC, Erdurman C, Durukan AH, Sobaci G, Bayraktar MZ. Acute effects of cigarette smoking on multifocal electroretinogram. *Clin Experiment Ophthalmol*. 2007;35:32–37.

Investigative Ophthalmology & Visual Science